JOURNAL OF MATERIALS SCIENCE 16 (1981) 604–612

Solidification path and phase equilibria in the liquid-solid range of cobalt-base alloy

C. GUYARD, A. BARBANGELO,* C. H. ALLIBERT, J. DRIOLE
Laboratoire de Thermodynamique et Physico-Chimie Métallurgiques, Associé au CNRS, Domaine Universitaire, 38401, Saint Martin d'Heres, France

For stellite 6 type alloys (Co–Cr–C–W), phase equilibria may be determined by several experimental methods, between liquidus and solidus temperatures. According to the composition of the different phases in this temperature range, two steps are found for the solidification path: from 1360 to 1280° C, a f c c solid solution based on Co–Cr crystallizes from the liquid phase; then, between 1280° C and the solidus temperature, the liquid phase meets and follows an eutectic line; at the same time, a eutectic precipitation of γ-phase and M_7C_3 takes place. Owing to the lack of diffusion of W in the solid phases, undercooling is observed at normal solidification rates.

1. Introduction

Some Co–Cr base alloys, commonly known as stellites, have found several specific applications such as in hard facing, owing to their excellent surface finish, hardness at high temperature and good corrosion resistance.

The microstructure of these materials has been extensively studied [1–4]. According to these rather old results, these alloys consist of a eutectic precipitation of a complex carbide in an austenitic matrix [5, 6]. Very often, rough dendritic microstructures are observed, resulting from a wide solidification range; as shown by Clemow and Daniell [7], they are related to substantial segregation of some alloying elements such as Cr. However, few quantitative results have been published on the composition of the phases present in the solidification process. We are interested in studying phase equilibria in the liquid–solid domain and the solidification path for a single alloy composed of Co, Cr, C, W, Si and Fe, known as stellite 6.

In spite of the large number of elements present in this material, some information on phase equilibria can be obtained by a survey of literature concerning the alloying behaviour of the main constituents Co, Cr, C and W. The Co–Cr binary system was established by Allibert *et al.* [8]. For the Co–Cr–C ternary system, the projection of solidification lines and one isothermal section at 800° C were plotted by Köster and Sperner [9]: these results are complemented by those obtained by Sahm *et al.* [10, 11] and Thompson *et al.* [12, 13] related to the unidirectional solidification of Co–Cr–C eutectic alloys. Regarding the effect of W, some data can be found from Knotek *et al.* [14] who determined two Co–Cr–W isothermal sections at 700 and 1050° C for two C contents.

The work that we carried out was a determination of the temperature range in which solidification takes place and the composition of phases existing between liquidus and solidus. The solidification trajectory can be deduced from these results.

2. Experimental procedure

2.1. Starting material

In order to avoid the strong segregation effects already mentioned, prealloyed powders obtained by inert gas atomization were used as starting material. Grain size was $< 36\,\mu m$; the chemical composition of the material is presented in Table I.

2.2. Experimental methods

First of all, liquidus and solidus temperatures were determined by differential thermal analysis. Alloys were contained in alumina crucibles and temperatures were measured using Pt–Rh 10%/Pt thermo-

*Present address: University of Genova, Genova, Italy.

0022–2461/81/030604–09$02.90/0

TABLE I Chemical composition of the starting powder (< 36 μm)

Composition	Co	Cr	C	W	Si	Fe	O_2	N_2
Atomic per cent	60.4	30.4	5.3	1.4	2.2	0.3	–	–
Weight per cent	64.3	28.6	1.15	4.65	1.	0.3	220 ppm	590 ppm

couples; experiments were performed under pure helium to prevent any changes in carbon content through oxidation.

The electromagnetic phase separation process [15, 16] was chosen to plot phase equilibria in the temperature range where the proportion of liquid phase was in excess of 50%. For differential thermal analysis (DTA), alumina crucibles, Pt–Rh/Pt thermocouples and helium at atmospheric pressure were employed. For each experiment, the working temperature was maintained for 2 h for the phases to reach equilibrium.

After cooling, all the elements of the "solid" phase were analysed with an electron microprobe.

For carbon analysis, two single phase alloys were prepared from Co, Cr and C; one part of each alloy was submitted to C analysis by high temperature vacuum extraction; the other part was used as a standard for the microprobe analysis.

The composition of the "liquid" phase was obtained by chemical analysis of the samples dissolved in acid solution.

In the temperature range where the proportion of the liquid phase is small, the electromagnetic process cannot provide a satisfactory separation. In this case, phase equilibria at several temperatures were determined by the rather unusual method of heating in a temperature gradient. A schematic diagram of the experimental device is presented in Fig. 1. The starting powder is poured into an alumina vessel which is placed in a horizontal alumina tube. This tube is heated by a resistor furnace which provides a temperature profile as shown in Fig. 2. The alumina vessel is located in the tube in such a way that a temperature range of 200° C exists from one end to the other. The furnace temperature is kept constant to within ± 1° C by regulation. A Pt–Rh 10%/Pt thermocouple enclosed in a gas-tight molybdenum sheath can be moved along the tube axis; consequently the vessel temperature can be measured every cm from one end to the other. During the experiments, 1 atm pressure of argon was supplied These experiments were performed for different heating times of 1, 2 and 5 h, between 1310 and 1110° C.

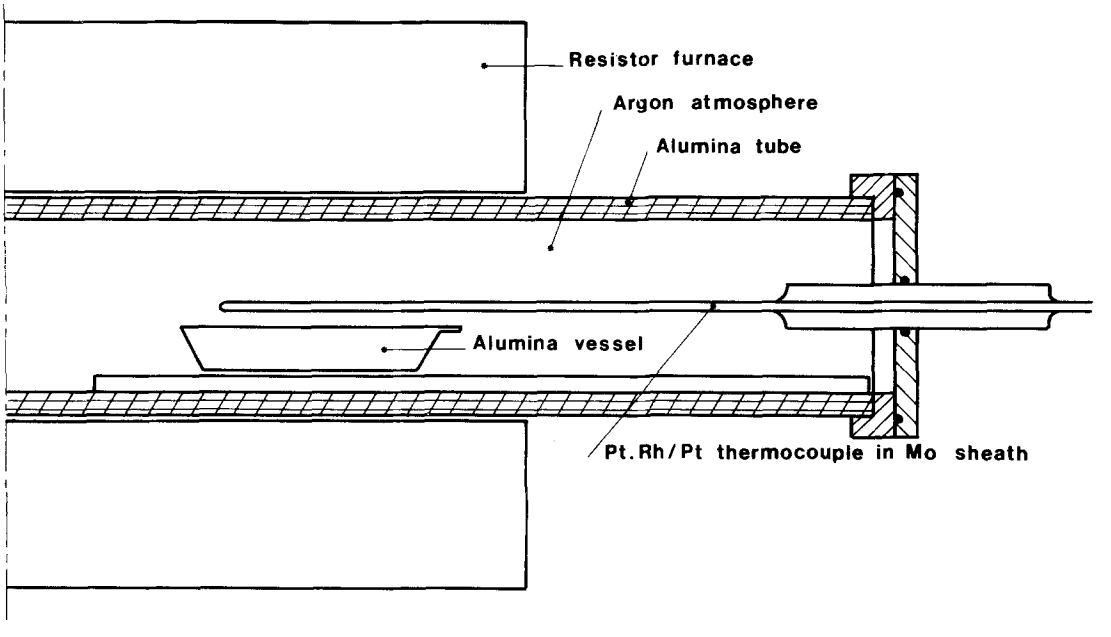

Figure 1 Schematic diagram of heating in a temperature gradient apparatus.

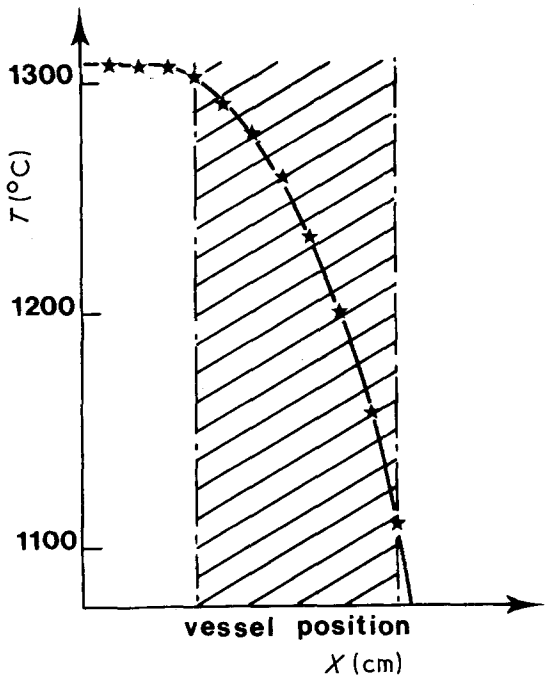

Figure 2 Temperature profile of the sample.

Such an experimental method can be used to describe phase equilibria in a well defined temperature range. Compared with unidirectional solidification, this method takes advantage of the possibility of prolonged duration in the temperature range concerned. This fact is very important when diffusion of some elements of the alloy is very slow, as we shall see for stellite.

3. Experimental results

3.1. DTA results

As already mentioned, fine prealloyed powders were used as starting material; the results obtained by DTA always show some discrepancy between the first heating curve, corresponding to the melting of the powder, and the subsequent ones relating to the melting of the cast structure.

3.1.1. First heating curves

Several experiments were carried out on powder, using heating rates from 400 to 100° C h^{-1}. In each case, two thermal effects were recorded and could be assumed to correspond to solidus and liquidus points. The upper thermal effect was found to be independent of the heating rate and was located at 1360 ± 4° C. The lower effect varied with heating rate, increasing from 1256 to 1272° C while the heating rate decreased from 400 to 100° C h^{-1}. As shown by these results, an accurate determination of the equilibrium solidus temperature is very difficult, some undercooling being observed even in the case of melting of prealloyed powders.

3.1.2. Cooling curves

From the cooling curves, two thermal effects were found with good reproducibility. The upper one, corresponding to the liquidus, is in good agreement with the heating results; the lower one is always located at 1280 ± 4° C, a temperature which is higher than the solidus temperature determined on heating. The first heating results indicate very easy undercooling of the liquid phase; under these conditions, on cooling, the solidus should occur at a lower temperature than on heating. Consequently, the thermal effect measured at 1280° C does not correspond to the liquidus but represents a monovariant point of solidification.

3.1.3. Subsequent heating curves

The heating curves were found to depend very little on the heating rates, showing a "solidification" solidus at about 1260° C and an equilibrium liquidus at 1360° C.

From a comparison of the different results obtained by DTA, it is shown that solidification of this alloy takes place in two steps: the first between 1360 and 1280° C and the second between 1280° C and a solidus temperature which is difficult to measure accurately. Undercooling is always observed in alloys obtained at normal solidification rates; in the case of prealloyed powders which exhibit very fine microstructures, it can be assumed that segregation, and consequently undercooling, is less and can diminish or disappear on slow cooling.

3.2. Electromagnetic phase separation (EPS) results

EPS results give the composition of phases in equilibrium in the first step of solidification. Six experiments were carried out in the temperature range 1360 to 1290° C. Fig. 3 represents a sample obtained at 1330° C; it can be seen that only two phases are found in equilibrium: one solid phase which is a fcc solid solution based on Co–Cr (γ-phase) and liquid phase. Compositions for each phase and each working temperature are presented in Table II. As shown in Fig. 3, some "liquid" phase is always retained in the grain boundaries; owing to its very fine microstructure, its total

Figure 3 Optical micrograph of a sample obtained by electromagnetic phase separation process at 1330° C (1) liquid phase, (2) "last liquid" phase and (3) solid phase (γ-Co–Cr).

composition can be obtained by microanalysis using an unfocused microprobe (8 to 10 μm probe diameter). Its composition is found to be the same for every small "island" dispersed in the solid part and gives an approximate value of the content of the "last liquid" during rapid solidification. According to these results, little γ-phase composition is produced on cooling, while the liquid phase becomes increasingly richer in C, Cr and W.

For each experimental temperature, the proportion of liquid (x) and solid (y) phase can be calculated by writing the atomic balance for each element, e.g. $x\,Co_l + y\,Co_s = Co_t$ and $x + y = 1$, where x is the liquid fraction, y the solid fraction, Co_l the cobalt content of the liquid phase, Co_s the cobalt content of the solid phase and Co_t the cobalt content of the starting material.

The values of x and y are reported in Table III. When x and y are calculated from Co or Cr atomic balances, they are in good agreement; but this is not the case when the C balance is used. Despite the reference to standards, it seems that microprobe analysis provides results lower than the true value for the C content of the γ-phase. It should be noted that such a discrepancy could be expected at this very low C level. In contrast good agreement between microanalysis and other analytical methods is found for higher C contents. Later the C content of the γ-phase will be calculated from x and y values.

In order to simplify, the solubility limit of each element in the liquid phase can be represented as a function of temperature by the following equations

$$\text{For Co} \quad \ln x_{Co_l} = 1.676 - 3.575 \times 10^3 \times \frac{1}{T}$$

$$\text{For Cr} \quad \ln x_{Cr_l} = -2.959 + 2.903 \times 10^3 \times \frac{1}{T}$$

$$\text{For C} \quad \ln x_{C_l} = -11.56 + 1.414 \times 10^4 \times \frac{1}{T}$$

$$\text{For W} \quad \ln x_{W_l} = -9.91 + 9.256 \times 10^3 \times \frac{1}{T},$$

TABLE II Composition of liquid and solid phases in equilibrium between 1350 and 1290° C.

Temperature (° C)	Phase	Composition (at %)						
		Co	Cr	C	$C_{calc.}$	W	Si	Fe
1350	Liquid	58.5	31.2	5.9	–	1.5	2.6	0.3
	Solid	69.1	26.9	0.2	0.33	1.1	2.4	0.3
1340	Liquid	58.2	31.4	6.1	–	1.6	2.4	0.3
	Solid	68.7	27.2	0.2	0.38	1.1	2.5	0.3
1330	Liquid	57.4	31.8	5.5	–	1.6	2.4	0.3
	Solid	68.5	27.2	0.2	0.78	1.1	2.6	0.3
1310	Liquid	55.7	32.6	7.4	–	1.7	2.3	0.3
	Solid	68.2	27.6	0.2	0.81	1.1	2.6	0.3
1290	Liquid	53.9	33.3	8.2	–	1.9	2.4	0.3
	Solid	68.0	27.7	0.2	1.0	1.1	2.7	0.3
	Last liquid*	44.6	35.4	16.2	–	1.6	2.0	0.2

*This "last liquid" composition corresponds to the mean of the value measured for each temperature, which are all very close together.

TABLE III Proportion of liquid phase, x, calculated from atomic balances of cobalt (x_l^{Co}) and chromium (x_l^{Cr})

Liquid fraction	Temperature (° C)				
	1350	1340	1330	1310	1290
x_l^{Co}	0.82	0.79	0.72	0.62	0.54
x_l^{Cr}	0.81	0.76	0.69	0.58	0.51

where x_l is the atomic fraction in liquid and T is the temperature in K. The lines corresponding to these equations are presented in Fig. 4.

Using these equations, we can calculate the composition of the liquid phase at 1280° C, which could not be obtained by any direct experimental method.

3.3. Heating in a temperature gradient

As shown by the DTA results, the solidification of stellite 6 occurs in two steps. By the EPS method, it was found that the first step corresponds to the crystallization of the γ-phase from a liquid; results obtained by heating in a temperature gradient confirm the EPS results and indicate that, during the second step, a eutectic precipitation of γ and M_7C_3 takes place while the liquid follows the eutectic curve down to the solidus.

Depending on temperature, several regions are observed in the sample (a) from 1110 to about 1220° C, the powder is not sintered and crumbles easily; (b) from 1220 to about 1250° C, sintering begins to take place, (c) from 1250 to 1280° C, the material is almost completely densified by liquid phase sintering; the closed porosity size is very small and (d) from 1280 to 1310° C, almost total sintering is obtained but the material collapses; the closed pores are coalesced and coarser than in the previous step.

Fig. 5 shows the microstructure corresponding to the different temperature zones. A clear change in morphology is found at about 1280° C, which is in good agreement with the DTA results. Another more diffuse change is observed between 1270 and 1260° C.

According to the EPS results, the microstructure observed in the 1310 to 1280° C zone represents dendrites of γ-solid solution in a liquid phase which crystallizes as a eutectic on cooling. Measured by microprobe analysis, the γ-phase composition agrees very well with the EPS results. In this experiment, cooling being rather slow, the eutectic structure related to the liquid phase is coarse and microanalysis with an unfocused probe is not possible for this eutectic part.

In the second zone (1280 to 1260° C), only γ-solid solution and M_7C_3* carbide seem to be present, but careful microprobe analysis reveals substantial W segregation localized on the edges of the γ-grains. This segregration corresponds to the white regions on the scanning electron micrograph (SEM) (Fig. 5b). It cannot be attributed to incomplete diffusion since it is not observed in the third zone where the temperature is lower. It cannot correspond to another solid phase since there is no grain boundary with γ-grains. Therefore, it must correspond to a liquid phase since we have already seen that the liquid phase is richer in W than the solid phase.

Consequently, in this part, 3 phases co-exist: γ, M_7C_3 and some liquid. Between 1280 and 1270° C, the liquid phase evolves along a eutectic curve and crystallizes as a γ–M_7C_3 eutectic. Because the proportion of liquid is small, on cooling this, precipitation occurs as a coherent layer on the solid phases present, as already shown in the W–Ni–Fe system [18] and does not appear as the usual eutectic morphology. From 1280 to 1260° C microanalysis detects a slight change of composition of γ and M_7C_3 solid phases; at the same time, the W segregations related to the liquid phase decrease.

In the third zone, that is to say below the solidus, γ and M_7C_3 are found; no more W segregation appears. Compared to the second zone, the microstructure is much finer, which can be explained by the fact that growth occurs by solid state diffusion which is slow.

The compositions of γ and carbide phases obtained by microprobe analysis are reported in Table IV. It must be noted that the composition change of Co, Cr and W in γ and M_7C_3 is small and only slightly greater than the accuracy limit. In order to make sure that the variation of the countings implies a compostion change, a large number of measurements were performed along the sample. A continuous trend was observed, indicating a decrease in Cr content and an increase in Co and W contents as the temperature decreased. As for the C content of the γ-phase at the solidus temperature, the value calculated from atomic

*The identification of the carbide phase, based on composition and structure analysis is described elsewhere [17].

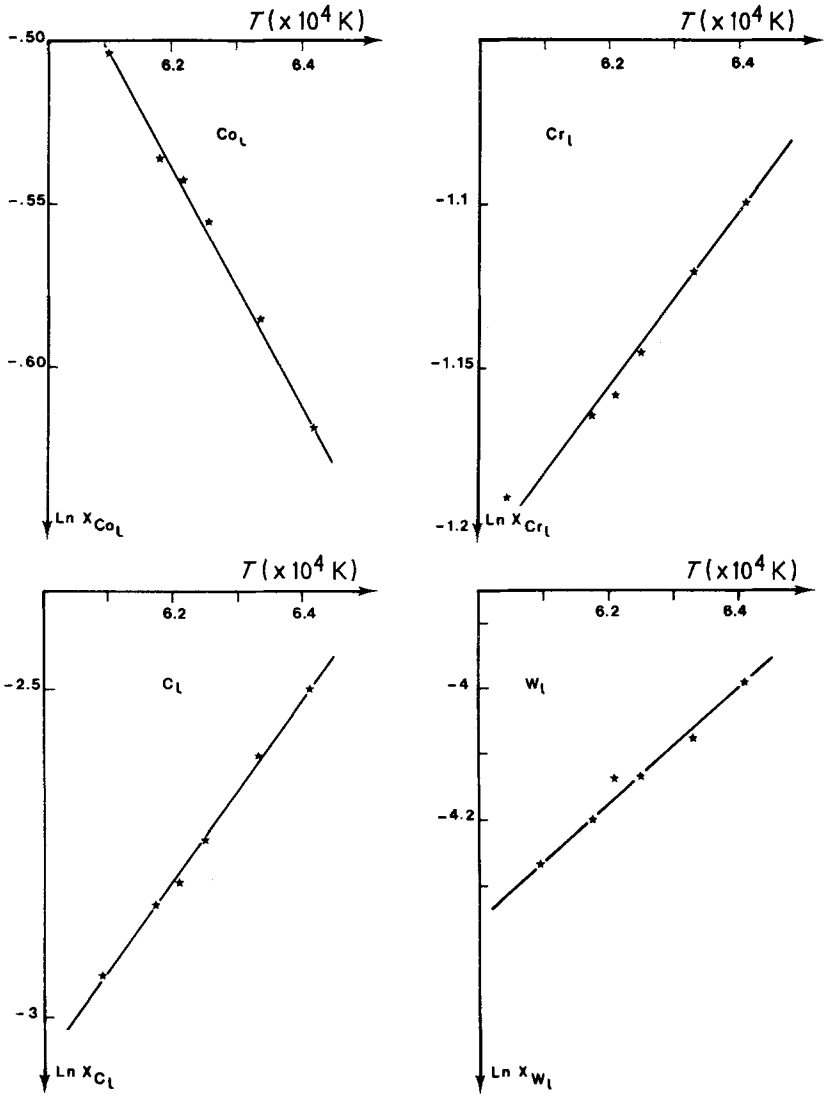

Figure 4 Solubility limit curves of Co, Cr, C and W in the liquid phase in equilibrium with the γ-solid solution.

balance (1.36 at %) as well as the value deduced by difference (1.2 at %) compare with the results published by Fritscher [19] who found 0.3 wt % (1.4 at %) for the maximum solubility of C in a γ Co–Cr–C solid solution. In the solid state, the proportion of γ and carbide is calculated from the atomic balance.

4. Interpretation of results

When 6 elements are present in the alloy, a simple representation of the solidification path and phase equilibria seems to be difficult. However, a comparison of previous results shows that Si and Fe contents are about the same in the liquid and solid phases as in the starting alloy and do not change with temperature. Consequently their level may be assumed constant, which would mean that only the change of other elements would need to be studied.

This sytem can be considered as a (Co, Cr, W, C) pseudoquaternary section with constant Si and Fe fraction values. Moreover, Cr and W fractions can be summed because these elements have the same crystal structure and are able to form a solid solution. Therefore, this alloy is represented as a pseudoternary ("C", "Co", "Cr + W") system for which the atomic fraction of each element is referred to the sum of the atomic fractions of C, Co, Cr and W.

It must be noted that the assumption of similar

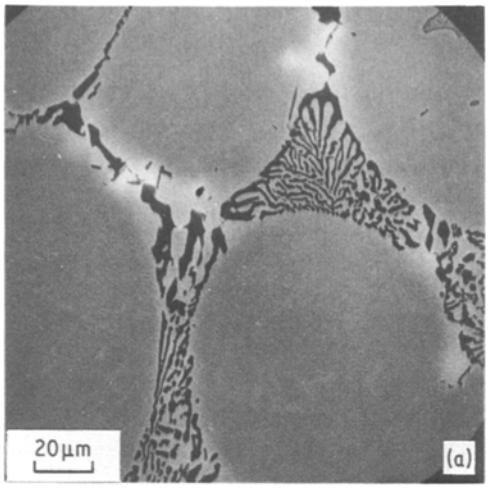

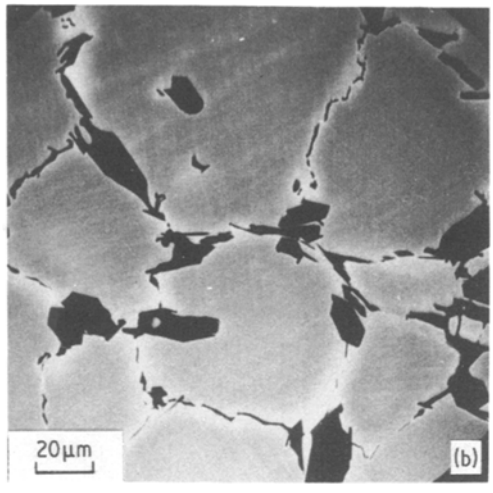

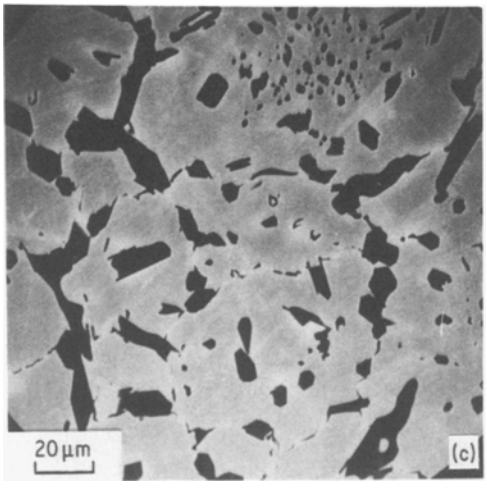

Figure 5 Scanning electron micrograph of a sample maintained for 5 h in a temperature gradient (a) between 1310 and 1280° C, liquid + γ-Co–Cr. (b) between 1280 and 1260° C, liquid + γ-Co–Cr + M_7C_3 and (c) between 1260 and 1230° C, γ-Co–Cr + M_7C_3. The microstructures observed in this case are produced by liquid phase sintering; they could not be obtained in a solidification process.

behaviour of Cr and W is valid for low W contents and would not necessarily hold for higher W levels; effectively, close to solidus, Cr and W exhibit an opposite trend in the solid phases. In the present case, the change of Cr and (Cr + W) fractions is always in the same direction, but it would not necessarily be the same for higher W contents. Using this model, a projection of the solidification path of this alloy is shown in Fig. 6. It can be seen that during the first step of solidification, the compositions of the solid and liquid phases change along the same AB line in the pseudo-ternary system; this means that when the temperature decreases, the tie-lines are parallel in the vertical plane containing AB, and the alloy behaves as a pseudobinary system. When the liquid reaches the eutectic trough (B point), the first carbide (C) which forms is out of line with the previous AB line. From this point on, γ changes from A to A′ and M_7C_3 from C to C′; A′C′ corresponds to the tie-line at the solidus temperature. We have little information on the liquid phase trajectory below 1280° C. However from a theoretical viewpoint, as soon as C (M_7C_3) forms, the liquid phase must change in the B″ direction to keep the initial point

TABLE IV γ-phase and M_7C_3 carbide compositions.

Temperature (° C)	Phase	Composition (at %)					
		Co	Cr	C	W	Si	Fe
1280	γ	67.3	27.7	(1.1)*	1.1	2.5	0.3
	M_7C_3	8.4	62.1	(29)*	0.5	nd	< 0.1
1260	γ	68.0	26.6	(1.2)*	1.4	2.5	0.3
	M_7C_3	9	61.1	(29.2)*	0.7	nd	< 0.1
	y_γ	0.88	0.88	–	–	–	–

*C content is calculated by difference.
nd: not detectable.

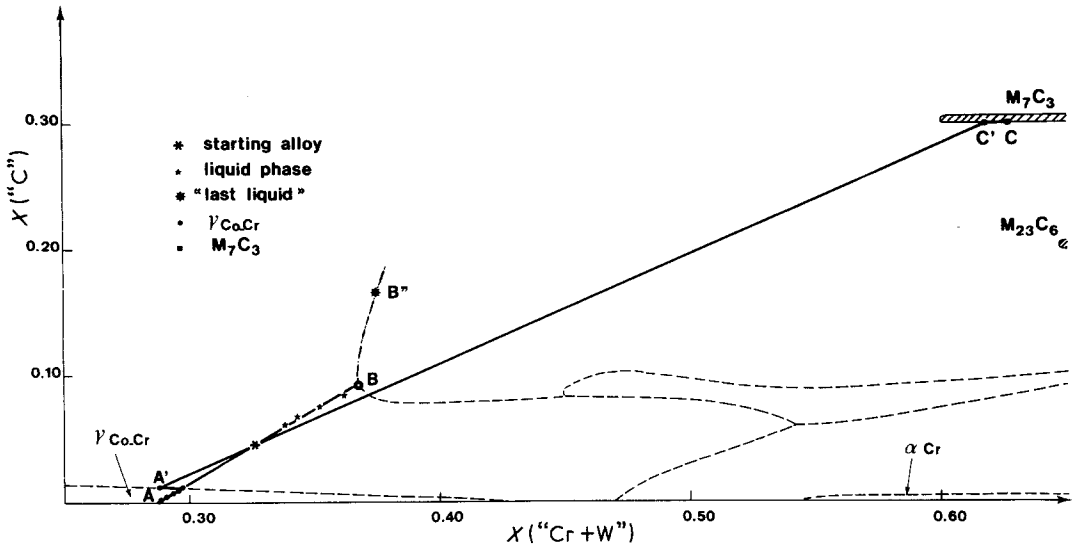

Figure 6 Projection of the solidification path of stellite 6. The dotted-lines correspond to the monovariant curves of the Co–Cr–C system from Koster and Sperner [9]; they only give qualitative information for the (C, Co, Cr + W) pseudoternary system.

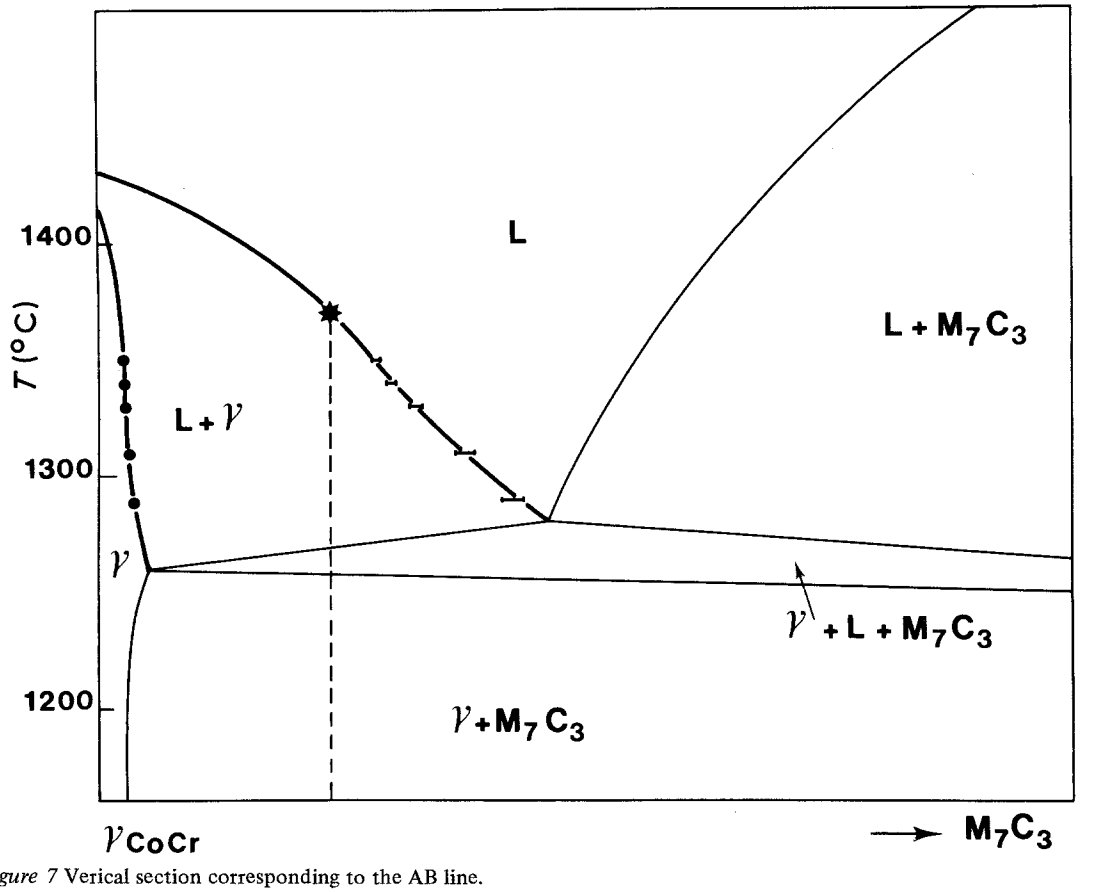

Figure 7 Verical section corresponding to the AB line.

inside the 3-phase triangle. The only experimental result corresponding to B″ agrees very well with this condition. Nevertheless, the B″ point obtained on fast cooling, can be rather far from the equilibrium point where the liquid phase must vanish. As mentioned earlier, the W content is higher in the liquid than in the solid phases; being very sluggish, the W diffusion from the liquid into γ and M_7C_3 is not completely achieved at the usual cooling rates and some liquid phase is retained by W supersaturation: this may explain the undercooling observed for most of the as-cast stellites and even in the case of prealloyed powders.

Another simple representation can be obtained by plotting the vertical section corresponding to the AB line (Fig. 7). In the temperature range 1360 to 1280° C, this section corresponds to a pseudobinary cut, and the tie-lines come from the EPS results. The other lines of the section are only a schematic representation because the study of a large number of compositions would be necessary to obtain quantitative information on the limits of the 3-phase triangle.

5. Conclusion

In spite of the large number of components, the solidification path of this alloy can be represented as a pseudoternary system (C, Co, Cr + W) and compares with the behaviour which could be expected from the examination of Co–Cr–C results previously published [9, 10, 12, 14]. Compared with the true ternary system where solidification can end when the liquid phase meets the eutectic line, W causes a second step of solidification along the eutectic line. Moreover, owing to its incomplete diffusion in the solid phases, W is responsible for undercooling, Up to now, we have not found any data in the literature on the effect of Si and Fe on the solidification of this alloy; consequently, it is not possible to know whether the simple pseudoternary representation which is presented would be valid for higher Si and Fe contents.

Acknowledgement

The authors thank Dr G. Raisson of the Research Centre of Imply SA who prepared the prealloyed powder of stellite 6 type alloy.

References

1. H. W. SHARP, *Welding J.* **25** (1946) 10, 936.
2. H. S. AVERY, *Iron Steel Eng.* **28** (1951) 81.
3. W. A. WISSLER, *Met. Prog.* **36** (1939) 131.
4. F. S. BADGER and F. C. KROFT, *ibid.* **52** (1947) 394.
5. B. LUX and W. BOLLMANN, *Cobalt* **12** (1961) 32.
6. D. COUTSOURADIS, *J. Int. Appl. Cobalt (Colloquium)* (1964) 1.
7. A. J. T. CLEMOW and B. L. DANIELL, *J. Biomed. Mater. Res.* **13** (1979) 265.
8. C. ALLIBERT, C. BERNARD, N. VALIGNAT and M. DOMBRE, *J. Common Met.* **59** (1978) 211.
9. W. KÖSTER and F. SPERNER, *Arch. Eisenhütten* **26** (1955) 555.
10. P. R. SAHM and D. J. WATTS, *Met. Trans.* **1** (1971) 1260.
11. P. R. SAHM, M. LORENZ, W. HUGI and V. FRÜHAUF, *ibid.* **3** (1972) 1022.
12. E. R. THOMPSON and F. D. LEMKEY, *ibid.* **1** (1970) 2799.
13. E. R. THOMPSON, D. A. KOSS and J. C. CHESNUTT, *ibid.* **1** (1970) 2807.
14. O. KNOTEK, H. SEIFAHRT and R. KIEFFER, *Arch. Eisenhütt* **39** (1968) 11.
15. C. ALLIBERT, J. DRIOLE and E. BONNIER, *Rev. Int. Hautes Temp. Réfractaires* **7** (1970) 45.
16. J. DRIOLE, C. ALLIBERT and E. BONNIER, *Metall.* **33** (1979) 5, 471.
17. C. GUYARD, S. THIBAULT and C. ALLIBERT to be published.
18. T. MARGARIA, C. ALLIBERT and J. DRIOLE, *J. Less Common Met.* **53** (1977) 85.
19. K. FRITSCHER, *Thermochimica Acta* **29** (1979) 357.

Received 19 June and accepted 18 July 1980.